ELSEVIER

Thermochimica Acta 332 (1999) 179–188

thermochimica acta

The temperature calibration on cooling of differential scanning calorimeters

J.A. Martins[a,*], J.J.C. Cruz-Pinto[b]

[a]*Departamento de Engenharia de Polímeros, Universidade do Minho, Campus de Azurém, 4800 Guimarães, Portugal*
[b]*Departamento de Química, Universidade de Aveiro, 3810, Aveiro, Portugal*

Abstract

The procedure for the calibration of differential scanning calorimeters (DSC) has been addressed by several authors. Most of the work published on this subject dealt mainly with the calibration on heating. For calibration on cooling, Menczel and Leslie suggested the use of thermally stable liquid crystals, for which the isotropic to nematic or cholesteric to isotropic transitions do not exhibit hysteresis on cooling. In this work, a new method is proposed to calibrate differential scanning calorimeters on cooling. It is suggested that the calibration on heating, with standard metals, may also be used to perform the calibration on cooling. The onset of the nematic to isotropic transition on heating (and vice-versa on cooling) will be used to support the method and to quantify the errors, which are of similar magnitude to those obtained by Menczel and Leslie with thermally stable high purity liquid crystals. Results of the change in the indium and lead crystallisation onset temperatures with the cooling rate are presented. Using as an example the non-isothermal crystallisation of polyethylene, the errors obtained with the standard calibration of the DSC and the new calibration on cooling are discussed.

Keywords: Scanning; Calorimeters; Calibration; Cooling

1. Introduction

To obtain meaningful results with a DSC, it is necessary to calibrate the device for both temperature and for heat (heat flow rate and/or peak area calibration) [1]. Discussions on how to perform the latter may be found elsewhere [1,2]. It is accepted that the temperature calibration is necessarily the result of two corrections: an isothermal correction to the measured temperature and a thermal lag [1,3,4]. The isothermal correction, calculated in the limit of zero heating rate [5], or by a stepwise melting of a high purity metal [1,3], essentially corrects the temperature measured by the sensor located at the bottom of the DSC cell. It will be shown in this work that, within the experimental errors, both of the above procedures will lead to the same results. The thermal lag may have two origins: one is due to the scanning rate and the other is dependent on the sample size (or mass) and geometry, as well as on its physical properties, being essentially the result of the thermal resistances of the DSC cell (and cover), sample pan (and cover) and sample. The use of the above corrections on heating and cooling will be discussed below.

The temperature calibration of differential scanning calorimeters is usually performed on heating because, for pure materials, it is possible to assign a definite value to their melting point. Recommendations on how to perform this calibration [5] and on the choice of the appropriate reference materials [6] have been

*Corresponding author. E-mail: zmartins@eng.uminho.pt

0040-6031/99/$ – see front matter
PII: S0040-6031(99)00072-6

published. When this calibration is performed (using a small mass of a high purity metal standard) at a fixed temperature scanning rate, and is then implemented on the DSC, the two effects referred to above, i.e., the isothermal correction and the thermal lag due to the scanning rate used, are automatically corrected for. If a high mass is being used, an additional temperature correction is needed, in order to take into account the effect of the additional thermal lag due to sample's thermal resistance.

Regarding the calibration on cooling of a DSC, to our knowledge, only two groups of authors have discussed the subject. Schick and Höhne [7] discussed possible symmetry in the temperature correction between the heating and the cooling modes. In their work, the temperature difference between the extrapolated onset measured on cooling, at a specified cooling rate, and the isothermal correction, plotted vs. the scanning rate, is shifted by the supercooling of the sample measured at nearly zero cooling rate. Data reported for the melting and crystallisation of indium (Fig. 1, [7]), at different scanning rates, corrected for the effects referred to above, show an obvious symmetry between the heating and cooling processes (see Fig. 7 below). Nevertheless, the authors' conclusion was that "for a power-compensated DSC, a symmetry in temperature correction between the heating and cooling mode is not valid". Of course, both the isothermal correction and the dependence of the measured temperature on the temperature scanning rate

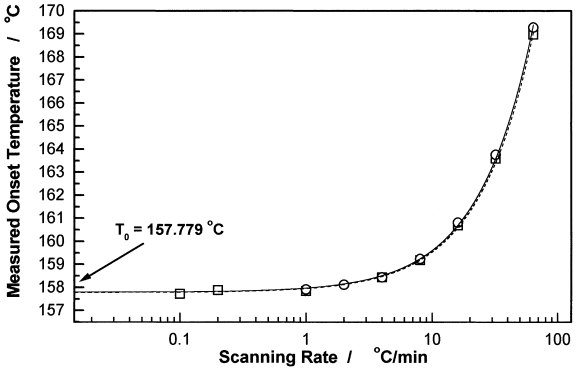

Fig. 1. Measured melting onset temperature vs. scanning rate, without calibration. Results for an indium sample with 8.143 mg and 99.99999 % pure, from Goodfellow. T_o is obtained from the (linear) plot of the onset temperature against the scanning rate.

are device-dependent. No data were reported so far concerning the accuracy of this calibration method.

Menczel and Leslie [8,9] discussed the calibration on cooling of power compensated DSCs, by using high purity (greater than 96%) liquid crystals. Recently, Menczel has extended the same procedure to heat-flux DSCs [10]. They concluded that several liquid crystalline transitions which have zero (or nearly zero) supercooling, can be used to calibrate a DSC on cooling. The precision of this calibration, reported by the authors, is 0.2°C for a scanning rate of 2°C/min, 0.7°C for 10°C/min, 1.7 for 20°C/min, 2.8 for 40°C/min and 6.6 for a scanning rate of 80°C/min [9].

In this work, a new method is presented to calibrate scanning calorimeters on cooling. It is proposed that the information obtained by the extrapolated temperature to the onset of the melting of a high purity calibration standard is essential for the calibration of a DSC on heating and can be used to calibrate a DSC on cooling [11]. The basis of the procedure and the experimental work are presented and discussed in the following sections of this report.

2. The calibration method

The corrections needed for the calibration of a DSC, either on heating or on cooling, are the isothermal correction, and a thermal lag due to the scanning rate and to the individual characteristics of the sample being analysed. However, despite the apparently simple way in which these corrections may be calculated, they deserve some discussion.

We first consider the ideal situation where the temperature sensor located at the bottom of the DSC cell is appropriately calibrated for isothermal experiments in the temperature range of interest. Here and in a conceptual experiment at *zero heating rate*, the temperature read by the sample holder temperature sensor (T_{sh}), for the melting onset of a small mass of a pure metal, should exactly match the expected (or true) temperature, i.e.,

$$T_t^+ = T_{sh}. \quad (1)$$

In a heating experiment at a *non-zero heating rate*, the temperature measured for the onset of melting of a small mass of a pure metal will deviate from the expected temperature, and this deviation will increase

with an increase of the heating rate. Thus, there will be a thermal lag between the sample and the sensor, but the measured temperatures (T_{sh}) can be corrected according to

$$T_t^+ = a_i^+ T_{sh} + b_i^+, \quad (2)$$

with appropriate a_i^+ (essentially independent of dT/dt) and b_i^+ (dT/dt – dependent) values. For a specific heating rate, those constants provide the corrections for the scanning rate thermal lag (provided that the temperature sensor is calibrated for an isothermal scan).

Additional corrections should also be performed in order to account for the individual characteristics of the sample: its mass and thermal properties. According to Richardson [1,12], these individual characteristics can be determined by performing an isothermal-scan-isothermal experiment and relating the area between the end of scan and the final isotherm to the sample mass and heat capacity. This procedure will enable the calculation of the thermal lag characteristics of that particular sample, which is also rate-dependent (Fig. 3, [12]). Extrapolation to a sample mass of zero gives a thermal lag that is due only to the scanning rate, and the temperature scale may be corrected by means of Eq. (2).

An alternative procedure to that proposed by Richardson may be used to calculate the sample's thermal lag. It is based on the evaluation of the sample's thermal resistance (R_s) and on the relation between the sample holder temperature, the true sample temperature and the heat flow rate [13,14]. This relation is given by equation

$$\Delta\dot{Q}^+ = \frac{1}{R_s}(T_{sh} - T_t^+), \quad (3)$$

where $\Delta\dot{Q}^+$ is the difference between the heat fluxes crossing the sample and reference ovens, during a heating scan.

When a small sample of indium (or other pure metal standard) is used for calibration and the calibration line is used to correct the temperature readings, the effect of the above thermal resistance is automatically accounted for.

However, if a sample of the same standard, of much higher mass, is used, its thermal resistance should be calculated and the temperature measured by the sample holder sensor corrected according to Eq. (3), or with the procedure proposed by Richardson. Also, if a polymer sample is used, its thermal resistance must be accounted for, using procedures given in the literature [14].

A common procedure is as follows: first, a small amount of indium is placed in an aluminium pan and melted at the scanning rate to be used in subsequent experiments, and for which the device is calibrated. The inverse of the slope of the ascending peak is the thermal resistance of the oven, aluminium pan and indium sample (± any difference in thermal contact resistance between this and the previous calibrating run). Next, the sample being analysed should be flattened to fit a similar aluminium pan. The indium sample used is carefully taken off from the pan and put above the sample and the pan sealed. The slope of the ascending part of this new indium peak will be different from the first one, as well as its onset temperature (Fig. 10). The difference between the inverse of the slopes is the thermal resistance of the sample.

Considering the thermal lags due to the *scanning rate* and *sample thermal characteristics*, the true sample temperature, for a *particular heating rate*, is

$$T_t^+ = a_i^+ T_{sh} + b_i^+ - R_s\Delta\dot{Q}^+. \quad (4)$$

In a cooling experiment, with the sensor calibrated for zero cooling rate (no isothermal correction needed), the same two thermal lag corrections are necessary and, as shown in Fig. 1, [7] and Fig. 3, [12], in a cooling experiment, they are symmetrical relative to those for a heating experiment.

For simplification, let us first consider a situation where the thermal lag due to the sample's thermal characteristics is negligible, the only important temperature correction being that due to the scanning rate. For a *non-zero heating rate*, the true sample temperature is always lower than the temperature measured by the sample holder sensor, i.e.

$$\Delta T^+ = T_t^+ - T_{sh} < 0, \quad (5)$$

and $|\Delta T^+|$ increases with the scanning rate. As referred to previously, for a particular scanning rate, this effect is accounted and duly corrected for by performing the calibration according to Eq. (2).

This being the only important effect, based on the working principle of the DSC, it is expected that, on cooling, the true sample temperature will be higher

than that of the sensor, i.e.

$$\Delta T^- = T_t^- - T_{sh} > 0. \quad (6)$$

Further, and still according to the same working principle, it is expected that, for a specified rate, the temperature difference on cooling will be equal in magnitude and opposite in sign to that on heating. In other words, the thermal lag on cooling will be symmetrical with that on heating [11],

$$\Delta T^- = -\Delta T^+, \quad (7)$$

and, from Eqs. (5)–(7), the calibration on cooling can be performed from the calibration on heating by

$$T_t^- = 2T_{sh} - T_t^+. \quad (8)$$

The calibration line on cooling is then, from Eqs. (2) and (8),

$$T_t^- = (2 - a_i^+)T_{sh} - b_i^+. \quad (9)$$

This equation is valid for the particular scanning rate used (the same for heating and cooling), and considers only the thermal lag due to the scanning rate.

The thermal lag due to sample characteristics may be corrected using the procedures referred to previously. The equation for cooling (similar to Eq. (3) for heating) is

$$|\Delta \dot{Q}^-| = \frac{1}{R_s}(T_t^- - T_{sh}), \quad (10)$$

where $|\Delta \dot{Q}^-|$ is the difference between the heat fluxes crossing the sample and reference ovens during a cooling experiment. The value of the sample's thermal resistance is the one calculated previously. The calibration line on cooling is then

$$T_t^- = (2 - a_i^+)T_{sh} - b_i^+ + R_s|\Delta \dot{Q}^-|. \quad (11)$$

The correction that remains to be introduced in Eqs. (2) and (4), for a heating experiment, and Eqs. (9) and (11), for a cooling experiment, is the *isothermal correction*. Once again, this correction is device-dependent. Its magnitude changes from one instrument to another, for the same DSC, it varies with changes in the external cooling block temperature, purge gas flow rate, the instrument's usage and also after any cell cleaning operations. For a particular DSC, it may be reduced by hardware to a nearly zero value, by adjusting specified trimpots, according to the manufacturer's instructions [15] – see Fig. 4 below. This offset may be calculated by plotting, before calibration, the measured onset of a calibration standard against the heating rate, and extrapolating to zero heating rate [5]. Another procedure, equivalent to this one, is to conduct a stepwise melting of the calibration standard [1,3,4]. Both procedures will yield similar results within the experimental errors (Figs. 1 and 3).

The isothermal correction should be the same for both modes, since it is due to an offset of the temperature read by the sensor located at the bottom of the sample holder (T_{sh}), although one may expect that it may vary slightly with the cell temperature. At zero heating (or cooling) rate, the difference between the measured value (T_m) and the value that should be read by the sample holder's sensor is

$$T_m - T_{sh} = \Delta T_o, \quad (12)$$

where ΔT_o is the isothermal correction. As a first approximation, in this work, it may be assumed to be a constant shift of the temperature read by the sample holder sensor.

The correction due to both the isothermal shift and the heating rate is then

$$T_t^+ = a^+ T_m + b^+ = a^+ T_{sh} + a^+ \Delta T_o + b^+, \quad (13)$$

where a^+ and b^+ may be different from those on Eq. (2) since, when a calibration is performed at a constant scanning rate, both of the above effects are automatically corrected for. The only effect that is not taken into account during a heating calibration is the thermal lag due to the sample characteristics. For a particular sample, and with the instrument calibrated for a particular heating rate, it may be corrected for according to Eq. (3). The calibration line including all of the effects referred to above is then

$$T_t^+ = a^+ T_m + b^+ - R_s \Delta \dot{Q}^+. \quad (14)$$

For the calibration on cooling, it must be remembered that the symmetry considerations that led to Eqs. (7) and (8) were applied to the correction of the thermal lag due to the scanning rate, and a correct temperature reading by the sample holder sensor was assumed. So, Eq. (8) will be used as a starting point to perform the calibration on cooling, where the substitution of Eq. (13) gives the true temperature on cooling as a function of the sample holder temperature

sensor,

$$T_t^- = (2 - a^+)T_{sh} - a^+\Delta T_o - b^+, \quad (15)$$

which must be expressed as a function of the measured temperature, as

$$T_t^- = (2 - a^+)T_m - b^-, \quad (16)$$

with $b^- = 2\Delta T_o + b^+$.

Taking into account the additional thermal lag due to the sample's characteristics, we finally have

$$T_t^- = (2 - a^+)T_m - b^- + R_s|\Delta\dot{Q}^-|. \quad (17)$$

An additional possible correction, shown in the Appendix A, is that due to a change of ΔT_o within the temperature range of interest.

3. Experimental

The DSC used in this work was a Perkin-Elmer DSC7 with the 7700 data system. Samples of two standards, indium and lead, from Goodfellow, with a purity of 99.99999% and 99.99% respectively, and a mass lower than 10 mg were sealed in aluminium pans. The liquid crystal used was from Merck, ref. CBOOA, and had the following chemical structure

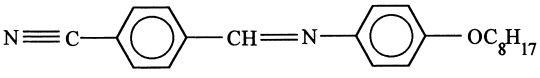

According to the manufacturer, the phase diagram of this material is

K - 78.8 - S_A - 83.0 - N - 107.0 - I.

A sample with a mass of 5.029 mg was placed in a aluminium pan identical to that used for the indium sample. The purity of this liquid crystal, measured by DSC, was 99.985%.

Two kinds of experiments were performed. In the first one, runs on heating and cooling with scanning rates from 1 to 64°C/min were performed with no calibration on the DSC. The information from the indium and lead melting onsets, at different heating rates, was used to perform the calibration on cooling. This set of data, as well as those for the liquid crystal, at the same scanning rates, were converted to ASCII data, and the calibration procedure was then tested using Eq. (13) for heating and Eq. (16) for cooling. In the second kind of experiments, the information obtained from the heating scans was used to calibrate the DSC on heating according to the procedure described on the DSC7 Perkin Elmer Manual [16]. A set of experiments on heating, at different heating rates and with different calibrations, were performed in order to check the accuracy of the calibration method. The calibration on cooling, performed according to Eq. (16), was also introduced in the DSCs data acquisition system, according to the usual calibration procedure. For this purpose, two fictitious standards were defined, with measured onset temperatures of e.g. 80 and 180°C, and the corresponding expected (true transition) temperatures were calculated by Eq. (16).

4. Results and discussion

Several runs on heating and cooling at scan rates from 0.1 to 64°C/min, were performed without any temperature calibration (the default DSC setting). Results for the change in the measured onset melting temperatures of indium and lead are shown in Figs. 1 and 2, respectively. Extrapolation to zero heating rate allows the calculation of the isothermal correction. Considering the melting temperature of indium and lead as 156.5985 and 327.47°C, respectively, that correction is $(\Delta T_o)_{In}$=1.1805°C and $(\Delta T_o)_{Pb}$= 1.539°C. Thus, in the temperature range defined by the melting temperatures of indium and lead, the isothermal correction changes by 0.3585°C. So, this

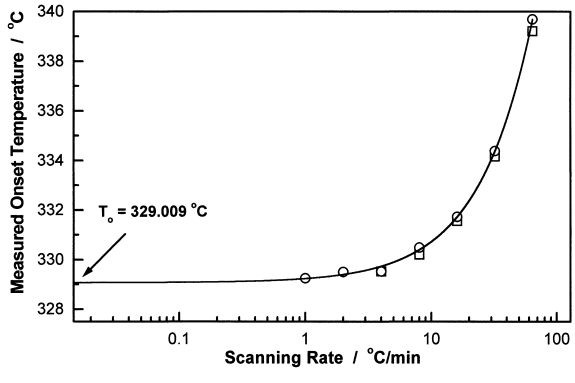

Fig. 2. Measured melting onset temperature vs. scanning rate, without calibration. Results for a lead sample with 5.055 mg and 99.99 % pure, from Goodfellow. T_o is obtained from the (linear) plot of the onset temperature against the scanning rate.

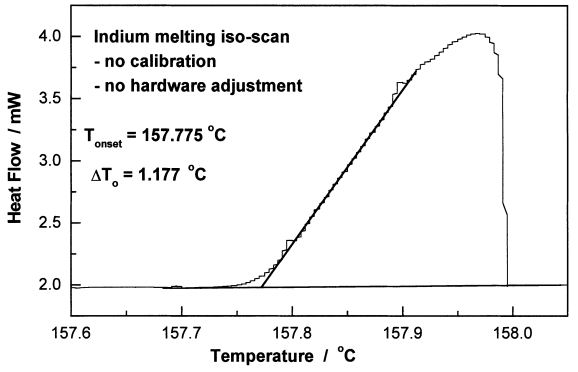

Fig. 3. Stepwise melting of an indium sample with baseline and without temperature calibration. The length of the isothermal step was of 30 s, and the rate of the scan step was 0.1°C/min. The temperature program was isothermal-heating ramp–isothermal-... .(sample mass 8.143 mg).

variation of the isothermal correction with temperature may be an additional source of error, unless this effect is appropriately taken into account.The magnitude of the isothermal correction may be measured either by the procedure used in Figs. 1 and 2, or by a stepwise melting, as shown in Fig. 3. The difference between the onsets measured by the two procedures is only 0.004°C, well within the experimental errors. This isothermal correction may be reduced by hardware to a lower value, as shown in Fig. 4. Two scans on an indium sample, at 0.1°C/min and by a stepwise melting, yield similar values for the onset melting

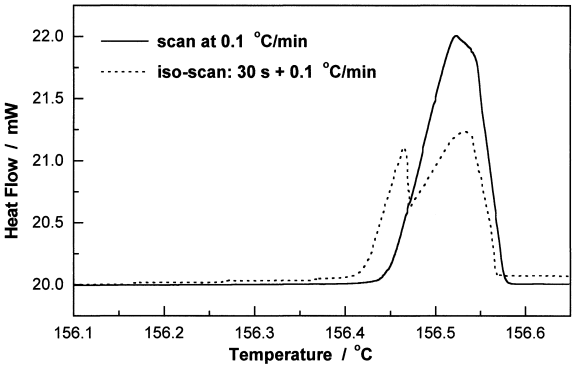

Fig. 4. Stepwise melting of an indium sample with baseline and without temperature calibration but after hardware adjustment (sample mass =3.220 mg). The length of the isothermal step was of 30 s and the rate of the scan step was 0.1°C/min. Comparison with a melting at 0.1°C/min (full line).

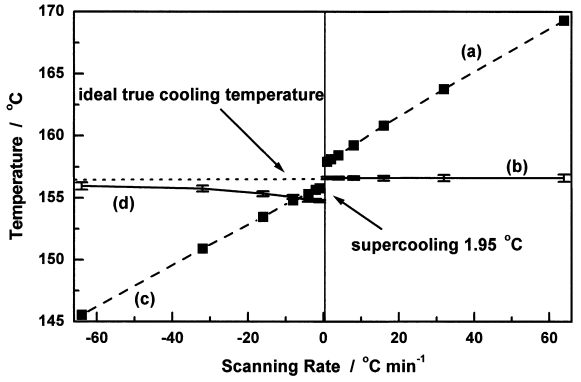

Fig. 5. Measured temperatures for indium melting and crystallisation at different scanning rates (sample mass=8.143 mg). (a) heating without calibration; (b) heating with calibration according to Eq. (13); (c) cooling without calibration; (d) cooling with calibration according to Eq. (16). *The ideal true cooling temperature* is the temperature that should be measured if the sample analysed had no supercooling and providing all the mentioned corrections were performed.

temperatures: 156.450°C and 156.422°C, respectively. In this case, the isothermal correction would be only 0.1765°C (taking as reference the value of the stepwise melting).

From the analysis of the data on Fig. 5, it may be concluded that there is an apparent symmetry in the thermal lag due to the scanning rate with respect to $(dT/dt)=0$. The data for indium in Fig. 5, illustrate the change of the measured temperature onset with the scanning rate on heating and cooling, without calibration – lines (a) and (c), respectively. A perfect symmetry between these lines is not expected since the above results need to be corrected for the isothermal lag; also, the results on cooling need corrections for the expected increase in the supercooling with the cooling rate. Lines (b) and (d) are the corrections of the measured onset temperatures during a heating scan, according to Eq. (13), and during a cooling scan, according to Eq. (16), respectively. In either lines (b) and (d) the corrections introduced are the isothermal correction and the thermal lag due to the scan rate. In both of these lines the error bars presented show the deviations between three independent runs and with the calibration introduced into the DSC. Since the mass of the sample used was very small, the corrections for the individual thermal characteristics of the sample are negligible. Line (d), however, shows an

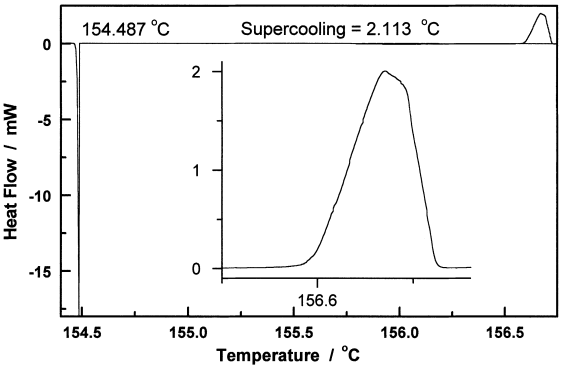

Fig. 6. Indium melting and crystallisation at 0.1°C/min, with calibration on heating according to Eq. (13), and calibration on cooling according to Eq. (16).

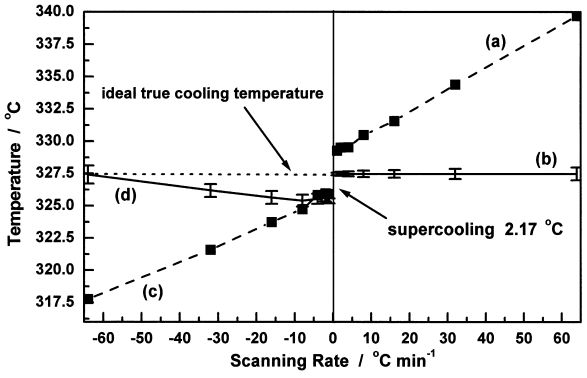

Fig. 7. Measured temperatures for lead melting and crystallisation at different scanning rates (sample mass=5.055 mg). Legend as in Fig. 5.

unexpected behaviour. In the limit of zero scanning rate, the supercooling is 1.95°C and it decreases with increasing scanning rates, while the opposite trend should be expected. The only possible explanation is the effect of experimental errors that can never be totally eliminated.

Concerning the above supercooling, a similar value, was obtained by performing scans on heating and cooling at scanning rates of 0.1°C/min, with the DSC calibrated on both modes according to Eqs. (13) and (16), respectively (Fig. 6). The value obtained was now 2.113°C. An also similar value, of 2.2°C, was previously obtained by Schick and Höhne [7]. Since in every liquid to solid transformation in pure metals there must be an supercooling, in order to form solid nuclei of size greater than or equal to the critical size [17], it is worth analysing the critical size of and indium nuclei formed at the supercooling measured. Assuming that the most probable shape for a stable nucleus is spherical, it may be derived that the critical radius is given by

$$r^* = \left(\frac{2\gamma_{SL}T_f^0}{\Delta H_f}\right)\frac{1}{\Delta T}, \qquad (18)$$

where γ_{SL} is the solid/liquid interfacial free energy (0.1777 J/m^2), ΔH_f is the heat of fusion (28.45×109 J/m^3), T_f^0 is the equilibrium melting temperature (in Kelvin) and ΔT the degree of supercooling. After substitution of the above values in Eq. (18), the resulting critical radius is 24.41 Å. Considering that the indium unit cell is tetragonal with a volume of 100×10^{-30} m^{-3}, the number of unit cells in the critical nuclei is ≈609 and the maximum number of indium atoms there presented is ≈2440 atoms. This is a reasonable value, since the maximum cluster size which occurs with reasonable probability in the liquid phase is of the order of ∼100 atoms [17].

The same explanation that was given for indium applies to lead (Fig. 7). In this case, the supercooling at the limit of zero cooling rate is 2.17°C. Using the same procedure as above, with the relevant values for lead (unit cell cubic, face centred, with a volume of 121.32×10^{-30} m^3, heat of fusion 21.32×10^9 J/m^3), gives critical nuclei with radii of ≈42 Å and containing approximately 2558 unit cells and ≈23027 atoms.

Some of the results obtained with the liquid crystal are presented in Figs. 8 and 9. Fig. 8 illustrates a check on the calibration procedure for the isotropic to nematic transition for a scanning rate of 1°C/min. Measurements of the heat capacity change across this transition show that it is first order and, therefore, the transition temperature should be measured at the peak onset and not at the maximum. The difference between the measured onset temperatures on heating and cooling is 0.257°C. On those data, no correction was performed considering the individual thermal characteristics of the sample, because the liquid crystal melts at a lower temperature than indium and therefore no information could easily be obtained on its thermal resistance. In Fig. 9, the same liquid crystal transition is presented, on heating and cooling with the calibrations introduced into the DSCs memory for a scanning

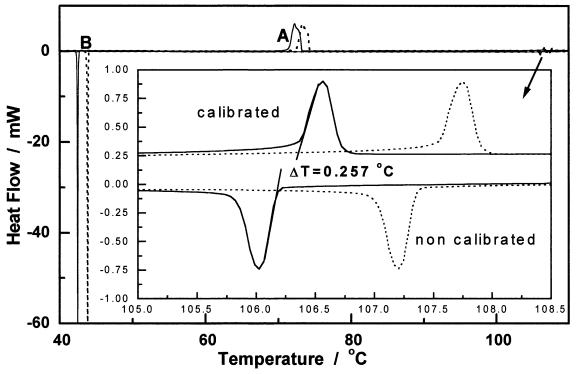

Fig. 8. Scan of the liquid crystal CBOOA at 1°C/min, without calibration and with calibration both on heating and cooling (sample mass=5.029 mg). These calibrations were performed using an ASCII data file. **A** is the crystal → smectic A transition and **B** is the reverse, greatly supercooled, S_A → crystal transition.

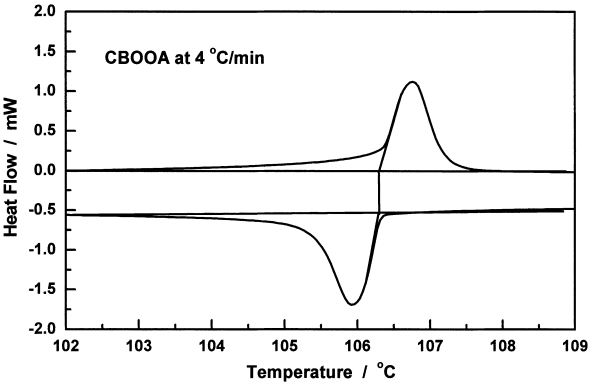

Fig. 9. Scan of the liquid crystal CBOOA at 4°C/min, with the calibrations on heating and cooling introduced in the DSC according to the manual's instructions. Results from ASCII data files yield the same deviation for the onsets. (See Table 1).

rate of 4°C/min. The difference between the onsets on heating and cooling is less than 0.15°C. Results for the deviations at other scanning rates, as well as the deviations between the corrected melting temperature and the calibrated crystallisation onset temperatures of indium and lead are presented in Table 1. To compare precision, the right-hand column of the table shows results obtained by Menczel and Leslie [9]. The magnitude of the errors is similar to ours. Also, the magnitude of the deviation from the true values increases with the cooling rate.

A possible explanation for the above results is that they may be due to the liquid crystal thermal resistance. As will be shown [18], in an isothermal scan (or at very low scanning rates), the temperature gradient between the temperature sensor and the sample is nearly zero (providing the enthalpy of the transition is not high), and, in such a scan, the thermal resistance of the DSC cell (and cover) and sample pan (and cover) may be neglected; also the thermal resistance of a small sample of high purity metal, of the order of 10^{-2} K/W, can be neglected [18]. The sample thermal lag is zero or negligible, and the difference between the measured onset temperatures on heating and cooling is due mainly to the finite supercooling of the sample. However, in a dynamic experiment, the temperature profile on the cell, pan, sample and cover is not linear, and these thermal resistances need to be considered to estimate the sample thermal lag. The thermal resistances of the cell, pan and cover are

Table 1
Values of the difference between the measured onset temperatures on heating and cooling after the calibration

dT/dt (°C/min)	In $T_t^+ - T_t^-$ (°C)	Pb $T_t^+ - T_t^-$ (°C)	CBOOA $T_t^+ - T_t^-$ (°C)	Menczel and Leslie $T_{real} - T_{ind}$ (°C)
1	1.872	2.092	0.257	−0.127
2	1.801	1.840	0.214	−0.200([a])
4	1.804	1.930	0.150	0.125
8	1.533	2.077	−0.029	0.460
16	1.269	1.823	−0.626	1.131
32	0.858	1.293	−2.250	2.472
64	0.649	0.066	−4.300	5.156

For each scanning rate a calibration was performed in both modes. The difference between the measured onset temperatures for the liquid crystal transition may be compared with those obtained by Menczel and Leslie. The value indicated with ([a]) was measured by the authors. The others are extrapolated from the values of the Table 1, [9]. T_{real} is the transition temperature measured by the calibrated instrument on heating (the same as T_t^+) and T_{ind} is the value measured for the transition temperature on cooling.

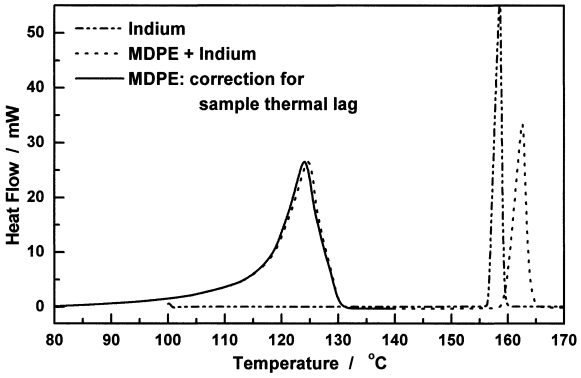

Fig. 10. Determination of the thermal resistance of a polyethylene sample (thickness=0.01 cm; area=0.3298 cm^2; sample mass=12.04 mg; sample resistance=23.021 °/W). All runs were obtained with temperature calibration on heating according to Eq. (13). Scanning rate=10°C/min.

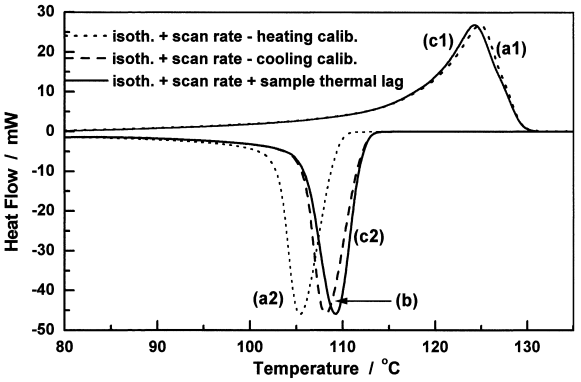

Fig. 11. 10.313 mg polyethylene sample scanned at 10°C/min. (a1) and (a2) calibration according to Eq. (13) – the same for heating and cooling; (b) calibration according to Eq. (16); (c1) and (c2) calibration on heating and cooling according to Eqs. (14) and (17), respectively.

automatically taken into account, when the calibration is performed on heating according to Eq. (2) or Eq. (13). The increase of the sample thermal lag with the scanning rate (heating or cooling) was already experimentally verified by Richardson [4,12].

The determination of the sample thermal resistance may be done according to the procedure described above in the Calibration Method (the same as in [14]). An illustration of the results obtained for a PE sample with a mass of 12.313 mg, flattened to fit a 25 µl aluminium pan, is shown in Fig. 10. The difference between the inverse of the slopes of the two indium peaks is the sample thermal resistance −23.021 °/W, for the case shown.

In Fig. 11, the change of a PE melting peak is also shown when the sample thermal resistance is considered. In the same figure, the effect of the calibration on cooling over the results obtained using the usual DSC calibration method on heating (Eq. (13)) is also shown: curve (a1) for heating and (a2) for cooling experiments. When the calibration is performed according to Eq. (16), the curve (a2) changes to (b). When the sample thermal resistance is considered, curve (a1) changes to (c1) Eq. (14) and (b) to (c2) Eq. (17), respectively. On heating, the effect of the sample mass does not appear to be significant. On the other hand, on cooling, all temperatures are shifted by approximately 5°C. The role of this effect on modelling the kinetics of non-isothermal crystallisation will be discussed in a separate report.

5. Conclusions

It is shown that the calibration on heating with standard metals may be used to calibrate the DSC on cooling, providing all corrections are taken into account: the isothermal correction, the thermal lag due to the scanning rate and the thermal lag due to sample's thermal resistance. Up to −10°C/min the error is less than 1°C. For high scanning rates this error increases and may reach values of 5°C or more. It is difficult, or even impossible, to quantify the exact value of the error for a calibration on cooling, the main reason being that, even for liquid crystals with a high purity, there may be a finite non-zero supercooling in the isotropic to nematic transition [19]. This supercooling may have a value of 0.4°C or even higher, depending on the purity of the liquid crystal. In addition, there are errors associated with the position of the sample in the DSC oven [20] and in the evaluation of its characteristic thermal lag. Considering all those difficulties, the proposed calibration method is acceptable within reasonable experimental errors.

Appendix A

In order to take into account the variation of the isothermal correction within the temperature range of interest, we take

$$\Delta T_o = a_o T_m + b_o, \tag{A1}$$

where T_m is the measured temperature for a specified scanning rate. The constants a_o and b_o may be determined from the measured onset temperatures for indium and lead, as

$$a_o = \frac{(\Delta T_o)_{Pb} - (\Delta T_o)_{In}}{T_{m,Pb} - T_{m,In}} \tag{A2}$$

and

$$b_o = (\Delta T_o)_{In} - a_o \cdot T_{m,In} = (\Delta T_o)_{Pb} - a_o \cdot T_{m,Pb}. \tag{A3}$$

Eq. (A1) may be introduced in Eqs. (13) and (14) for heating, and in Eqs. (16) and (17) for cooling, in order to take into account the effect described above.

References

[1] M.J. Richardson, in: G. Allen, A. Bevington (Eds.), Comprehensive Polymer Science, vol. 1, Pergamon Press, Oxford, 1989, p. 867.
[2] S. Sarge, E. Gmelin, G.W.H. Höhne, H.K. Cammenga, W. Hemminger, W. Eysel, Thermochim. Acta 247 (1994) 129.
[3] J.H. Flynn, Thermochim. Acta 8 (1974) 69.
[4] M.J. Richardson, N.G. Savill, Thermochim. Acta 12 (1975) 213.
[5] G.W.H. Höhne, H.K. Cammenga, W. Eysel, E. Gmelin, W. Hemminger, Thermochim. Acta 160 (1990) 1.
[6] H.K. Cammenga, W. Eysel, E. Gmelin, W. Hemminger, G.W.H. Höhne, S. Sarge, Thermochim. Acta 219 (1993) 333.
[7] C. Schick, G.W.H. Höhne, Thermochim. Acta 187 (1991) 351.
[8] J.D. Menczel, T.M. Leslie, Thermochim. Acta 166 (1990) 309.
[9] J.D. Menczel, T.M. Leslie, J. Thermal Anal. 40 (1993) 957.
[10] J.D. Menczel, J. Thermal Anal. 49 (1997) 193.
[11] J.A. Martins, Cristalização de Polímeros: Estudo Experimental e Modelação Teórica, PhD Thesis (1996) Universidade do Minho, Braga, Portugal.
[12] M.J. Richardson, Thermochim. Acta 300 (1997) 15.
[13] J. Shawe, C. Schick, Thermochim. Acta 187 (1991) 335.
[14] V.A. Bershtein, V.M. Egorov, Differential Scanning Calorimetry of Polymers: Physics, Chemestry, Analysis, Technology, Ellis Horwood Series in Polymer Science and Technology, 1994, p. 10.
[15] DDSC-7 system, Instalation Manual, Perkin Elmer (1995).
[16] DSC7 Differential Scanning Calorimeter Manual, Perkin Elmer (July 1990) Sect. 8.
[17] D.A. Porter, K.E. Easterling, Phase Transformations in Metals and Alloys, Van Nostrand Reinhold (UK) Co. Ltd, 1987, chapter 4.
[18] J.A. Martins, J.J.C. Cruz Pinto, to be submitted.
[19] N. Oranth, F. Strhbusch, Ber. Bunsenges. Phys. Chem. 91 (1987) 211.
[20] G.W.H. Höhne, E. Glöggler, Thermochim. Acta 151 (1989) 295.